CHEMICAL ENGINEERING TRANSACTIONS
VOL. 94, 2022
A publication of AIDIC
The Italian Association of Chemical Engineering
Online at www.cetjournal.it
Guest Editors: Petar S. Varbanov, Yee Van Fan, Jiří J. Klemeš, Sandro Nižetić

ISBN 978-88-95608-93-8; **ISSN** 2283-9216
DOI: 10.3303/CET2294041

Multiphysics Modeling of a Low Voltage Acid-Alkaline Electrolyzer

Michael T. Castro[a], Po-Ya Abel Chuang[b], Joey D. Ocon[a,*]

[a] Laboratory of Electrochemical Engineering, Department of Chemical Engineering, University of the Philippines Diliman, Quezon City 1101, Philippines
[b] Thermal and Electrochemical Energy Laboratory (TEEL), Department of Mechanical Engineering, University of California, Merced, California, 95343, USA
jdocon@up.edu.ph

Acid-alkaline electrolyzers utilize an acidic catholyte and alkaline anolyte, which lower the thermodynamic voltage requirement for water splitting. Experiments have demonstrated the feasibility of acid-alkaline electrolyzers with proton exchange membranes, but a mathematical model has yet to be developed to understand their operation. This work developed a multiphysics model of a batch acid-alkaline electrolyzer with a H_2SO_4 catholyte, a NaOH anolyte, and a proton exchange membrane. The model was formulated in COMSOL Multiphysics® and validated using experimental current vs. voltage data in literature. The electrolyzer's reactions and ion transport were analyzed based on the electrolyte potential, concentration profiles, and ion fluxes calculated by the model. The charge imbalance due to the consumption of H^+ and OH^- in the catholyte and anolyte, respectively, is addressed by Na^+ transport from the anolyte to the catholyte. This contradicts the prevailing hypothesis that electroneutrality in a proton exchange membrane acid-alkaline electrolyzers is preserved by the Second Wien Effect, or water splitting in high electric fields. H^+ is transported from the catholyte to the anolyte, which results in undesired acid-base neutralization. This is minimized by increasing the applied voltage, which shows a tradeoff between power and reactant consumption. Na^+-selective membranes also hinder the neutralization reaction, but their realization is challenging due to the smaller Stokes radius of H^+. The proposed model can be used to optimize the parameters of a batch electrolyzer and aid in the design of a continuous electrolyzer stack.

1. Introduction

The rising awareness on greenhouse gas emissions from fossil fuels has prompted the search for a more sustainable energy carrier. Hydrogen is viewed as one such alternative since it can be generated via water electrolysis powered by renewable energy (Tufa et al., 2017) and yields water as the sole emission after use. Unfortunately, the widespread application of water electrolysis is hindered by the high thermodynamic voltage requirement of the water splitting reaction and the sluggish kinetics of the oxygen evolution reaction, which must occur in tandem with hydrogen generation (Kumar et al., 2021).

Acid-alkaline electrolyzers are an innovative approach in lowering the voltage requirement of water electrolysis. Electrolyzers that employ a single electrolyte have a thermodynamic voltage requirement of 1.23 V for water splitting. On the other hand, acid-alkaline electrolyzers contain an acidic catholyte and alkaline anolyte, which lowers the thermodynamic voltage requirement to 0.401 V (Weng and Chen, 2016). The two half-cells must be separated by a semipermeable membrane to prevent the unwanted acid-base neutralization reaction.

Bipolar exchange membranes (BEM) are typically used in acid-alkaline electrolyzers. These consist of cation exchange membranes (CEM) and anion exchange membranes (AEM) laminated together. The CEM and AEM face the catholyte and anolyte, respectively. When a potential is applied to the electrolyzer, a large electric field forms at the CEM-AEM interface, which splits water into H^+ and OH^- (Zhang et al., 2020). The ions are transported to the catholyte and anolyte, respectively, to replace the ions consumed in the hydrogen (HER) and oxygen evolution reactions (OER) (Zhang et al., 2020). The high potential drop across the membrane, however,

Paper Received: 01 April 2022; Revised: 21 April 2022; Accepted: 30 April 2022
Please cite this article as: Castro M.T., Chuang P.-Y.A., Ocon J.D., 2022, Multiphysics Modeling of a Low Voltage Acid-Alkaline Electrolyzer, Chemical Engineering Transactions, 94, 247-252 DOI:10.3303/CET2294041

results in low current densities and requires the use of water splitting catalysts at the CEM-AEM interface (Zhang et al., 2020), in addition to the HER and OER catalysts.
A lesser-known alternative to BEMs is proton exchange membranes (PEM), which do not require additional catalysts for water splitting. Weng and Chen (2016) were the first to demonstrate that PEMs can be used to separate the anolyte and catholyte in an acid-alkaline electrolyzer. They were also able to achieve water splitting at 0.8 V, which was lower than the voltage requirement of BEM electrolyzers. Zhu et al. (2018) also used a PEM to construct an acid-alkaline electrolyzer, although their work focused more on showcasing HER and OER catalysts based on a zeolitic imidazolate framework. Despite the promising characteristics of PEM acid-alkaline electrolyzers, however, the operating mechanism (i.e., reactions and ion transport) are unknown.
In this work, a multiphysics model for a PEM acid-alkaline electrolyzer was proposed to reveal the key reactions and ion transport mechanisms. The model was formulated in COMSOL Multiphysics® based on the electrolyzer constructed by Weng and Chen (2016) and validated with experimental voltage vs. current data from the same study. The reactions and ion transport mechanisms that occur in the electrolyzer were then determined from the electrolyte potential and concentration profiles calculated by the multiphysics model. Lastly, a sensitivity analysis was performed to find possible improvements to the electrolyzer. This study is the first to investigate the operating mechanism behind the acid-alkaline electrolyzer, and the first to propose a model for it.

2. Methodology

This section discusses the experimental setup of the acid-alkaline electrolyzer, the formulation and validation of the multiphysics model, and the case studies performed to investigate the acid-alkaline electrolyzer.

2.1 Experimental setup

The PEM acid-alkaline electrolyzer reported by Weng and Chen (2016) consists of a 0.1 cm^2 Pt cathode, a 1 cm^2 NiFe LDF anode, 0.5 M H_2SO_4 catholyte, and 1 M NaOH anolyte is considered in this study. Their work highlights the use of CoP cathodes due to their low cost, but their setup with Pt cathodes had clear pseudo-steady-state voltage vs. current behavior, which is useful for validating the model.

2.2 Proposed mechanisms

The possible reactions and ion transport in the electrolyzer are presented in Figure 1. The catholyte and anolyte contain H^+ and OH^-, which are consumed by the HER and OER, respectively. The loss of charged ions results in a net charge, which must be addressed by an electroneutrality mechanism. One possible phenomenon is the Second Wien Effect, or the splitting of water into H^+ and OH^- under a large electric field, which maintains electroneutrality in a BEM acid-alkaline electrolyzer. This would be more significant at the membrane-anolyte interface since OH^- would remain in the anolyte, while H^+ would be transported to the catholyte. Alternatively, the crossover of Na^+ and sulfate ions to their opposite half-cells may also preserve electroneutrality. As for side reactions, acid-base neutralization may occur if H^+ and OH^- crossover into the opposite half-cell.

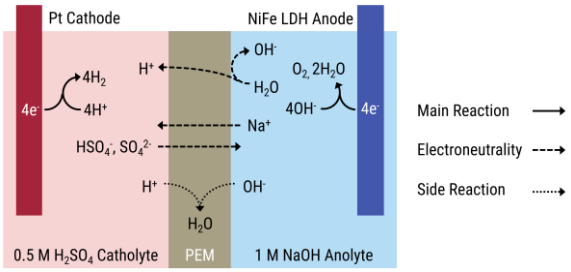

Figure 1: Possible reactions and ion transport in a PEM acid-alkaline electrolyzer

2.3 Multiphysics model

The 1D multiphysics model of the PEM acid-alkaline electrolyzer is illustrated in Figure 2. A 1D model considers only the electrolyte within the space defined by the cross-sectional area and the cathode to anode distance. This fails to consider the rest of the electrolyte. An ion generation term $R_{\mathrm{rep},i}$ is therefore introduced as shown by Eq(1). Each ion i replenishes faster as its concentration difference with the bulk electrolyte $c_{\mathrm{b},i}$ becomes larger. The bulk electrolyte concentration is assumed equal with the initial electrolyte combination, which permits a pseudo-steady-state operation. The replenishment constant k_{rep} represents the rate at which ions in the 1D model are replenished by the bulk electrolyte.

$$R_{\mathrm{rep},i} = -k_{\mathrm{rep}}\left(c_i - c_{\mathrm{b},i}\right) \quad (1)$$

The experimental setup also utilizes electrodes with different surface areas. A 1D model assumes a uniform cross-sectional area, so the unequal areas are accounted for by scaling the cathodic current by a factor of 0.1.

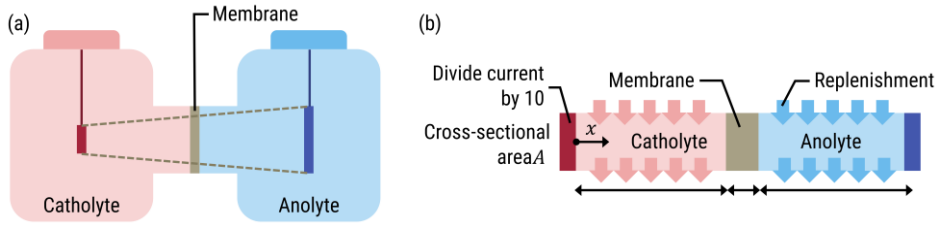

Figure 2: Illustration of the experimental setup (a) and conversion into 1D multiphysics model (b)

HER and OER are described by Butler-Volmer kinetics. Ion transport is modeled by the Nernst-Planck-Poisson equations. The Poisson equation ensures a differentiable electrolyte potential at the electrolyte-membrane interfaces, thereby allowing the calculation of the electric field, which is the negative gradient of the electrolyte potential. The electric field is required for modeling the Second Wien Effect, as given by Eq(2), which explains how the water dissociation equilibrium constant K_w increases with the magnitude of the electric field $|E|$ (Eckstrom and Schmelzer, 1939). Complete dissociation of H_2SO_4 was assumed, while those of water and HSO_4^- were given by their respective equilibrium constants. All ions may cross the PEM, but the diffusion coefficients in the membrane are different and favor the transport of H^+. The Poisson equation also accounts for the presence of fixed charged sites in the membrane.

$$\frac{K_w}{K_{w,0}} = \frac{J_1\left(\sqrt{8bi}\right)}{\sqrt{2bi}} \quad b = (0.09636\ \mathrm{K^2\ m\ V^{-1}})\frac{|E|}{\varepsilon_r T^2} \quad (2)$$

2.4 Input model parameters

The domain-specific input parameters to the multiphysics model are presented in Table 1, while the diffusion coefficients of ions in the aqueous solution and the membrane are shown in Table 2. The PEM membrane was not specified in the work of Weng and Chen (2016), so it was assumed to have the same properties of Nafion™ 115. The electrode-membrane distance was also unknown, so it was fitted to match the experimental pseudo-steady-state voltage vs. current data.

Table 1: Domain-specific input parameters to the model

Parameter	Cathode	Membrane	Anode
Initial H^+ concentration [mol m^{-3}]	511.37 [a]	1200 [*]	0
Initial HSO_4^- concentration [mol m^{-3}]	488.63 [a]	0	0
Initial SO_4^{2-} concentration [mol m^{-3}]	11.37 [a]	0	0
Initial Na^+ concentration [mol m^{-3}]	0	0	1000 [a]
Initial OH^- concentration [mol m^{-3}]	0	0	1000 [a]
Replenishment constant [s^{-1}]	10 [*]	0	10 [*]
Length [cm]	1.4636 [†]	0.0125 [b]	1.4636 [†]
Fixed site concentration [mol m^{-3}]		1200 [c]	
Equilibrium potential [V]	0		0.401
Exchange current density [A m^{-2}]	3.5405 [†]		0.00811 [†]

[*] Assumed [†] Fitted to experiment [a] (Weng and Chen, 2016) [b] (Jiang et al., 2016) [c] (Wang et al., 2014)

Table 2: Diffusion coefficients of the ions in the solution and membrane

Diffusion coefficient	Na^+	HSO_4^-	SO_4^{2-}	H^+	OH^-
In aqueous solution [10^{-9} m^2 s^{-1}]	1.334 [a]	1.385 [a]	1.065 [a]	9.311 [a]	5.273 [a]
In the PEM [10^{-9} m^2 s^{-1}]	0.1580 [b]	0.0400 [c]	0.0011 [b]	0.3500 [c]	0.0456 [d]

[a] (Haynes, 2012) [b] (Stenina et al., 2004) [c] (Agar et al., 2014) [d] (Piela and Wrona, 2006)

2.5 Case studies

Two case studies are considered in this work: a base scenario and a sensitivity analysis. In the base scenario, the multiphysics model was simulated under applied voltages from 0.8 V to 1.2 V with the default input parameters. Ion flux profiles, electric fields, and overpotentials were computed, and the key reactions and ion transport mechanisms were inferred. The sensitivity analysis was performed by varying the Na^+ and H^+ diffusion coefficients in the PEM by factors from ×0.1 to ×10 at 1.0 V applied voltage. This determines how the PEM should be modified for acid-alkaline electrolyzers.

3. Results and discussion

This section presents the experimental validation of the multiphysics model, followed by the simulation results under the base scenario and the sensitivity analysis.

3.1 Experimental validation

Figure 3 compares the pseudo-steady-state current vs. voltage predicted by the model and obtained from the experiment. The model generally shows good agreement since the electrode-membrane distance and kinetic parameters were fitted to match experimental data. A slight deviation is observed at 0.8 V, which is likely due to the formation of bubbles. Ohmic drop due to bubble formation is not explicitly considered in the model, but its effects may be captured in the fitted electrode-membrane distance, which also results in an ohmic potential drop. Discrepancies due to bubbles would therefore be more notable at lower voltages, since this is where overpotentials due to bubbling resemble activation losses instead of ohmic drops (Chen et al., 2017).

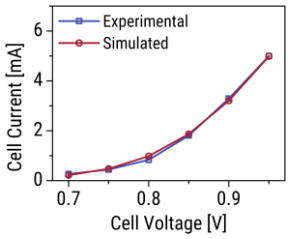

Figure 3: Comparison between experimental and simulated current vs. voltage

3.2 Base scenario

Figure 4a shows the electric field in the electrolyzer, which is maximum at the electrolyte-membrane interfaces.

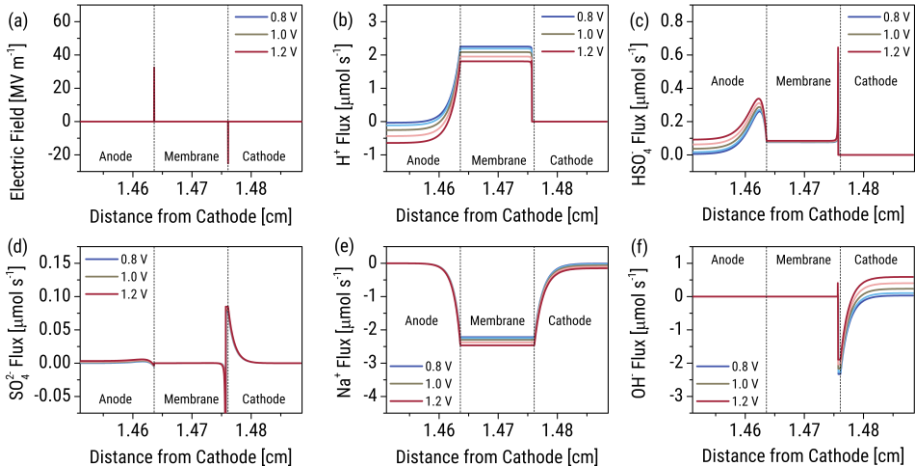

Figure 4: Electric field (a), and ion flux profiles of H^+ (b), HSO_4^- (c), SO_4^{2-} (d), Na^+ (e), and OH^- (f) at applied voltages from 0.8 V to 1.2 V

This is due to the Donnan effect, or the sudden shift in electrolyte potential across an ion-selective membrane (Macgillivray, 1968). Figures 4b-4f present the ion fluxes near the membrane. H^+ ions are transported to the cathode to produce H_2 gas, but they are also transported to the anolyte and contribute to the undesired acid-

base neutralization reaction. Similarly, OH^- ions migrate to the anode for O_2 generation, but acid-base neutralization also occurs in the membrane. Na^+ crossover from the anolyte to the catholyte occurs in notable quantities, suggesting that it contributes to retaining electroneutrality. The sulfate ions are also transported to the opposite half-cell to retain electroneutrality, but in much smaller amounts since a PEM is cation selective.
Figure 5a shows the electric field at the electrolyte-membrane interfaces at various applied voltages. It can be observed that electric fields in the electrolyzer are not large enough to significantly alter K_w. For reference, a 10-fold increase in K_w, which is still too small, requires an electric field of 229 MV/m. The Second Wien Effect is therefore negligible in the electrolyzer, and that Na^+ crossover is the dominant electroneutrality mechanism. This has unfortunate consequences on the practicality of PEM acid-alkaline electrolyzers. If the Second Wien Effect were the primary electroneutrality mechanism, then the electrolyzer would only require water as fresh feed. The crossover of Na^+, however, implies that cross-contamination occurs between the catholyte and anolyte, so fresh H_2SO_4 and NaOH must be fed to the electrolyte after each use. Figure 5b shows the crossover of ions to the opposite half-cell. At higher applied voltages, the crossover of Na^+ increases, while the crossover of H^+ decreases. Raising the applied voltage therefore inhibits the acid-base neutralization reaction in favor of HER and OER. This, however, demonstrates a tradeoff between power and reactant consumption: a lower applied voltage lessens the power consumption but results in reactant wasted due to acid-base neutralization. Conversely, a higher applied voltage increases the power draw but minimizes the amount of wasted reactant. The overpotentials are shown in Figure 5c. Activation overpotentials are significant at lower applied voltages, but ohmic overpotentials catch up at higher applied voltages.

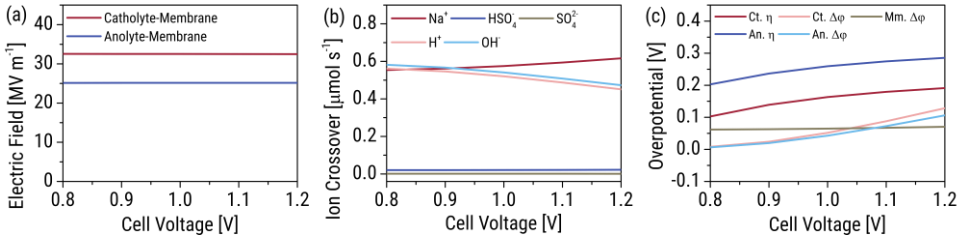

Figure 5: Electric fields at the electrolyte-membrane interfaces (a), ion crossover (b), and activation η and ohmic $\Delta\phi$ overpotentials (c) at applied voltages from 0.8 V to 1.2 V

3.3 Sensitivity analysis

Figure 6 presents the effect of varying the Na^+ and H^+ membrane diffusion coefficients on the performance of the electrolyzer. Raising the Na^+ diffusion coefficient increases the cell current and Na^+ crossover, but this also promotes H^+ crossover, and consequently, the acid-base neutralization reaction. In contrast, decreasing the H^+ diffusion coefficient, which is equivalent to raising the Na^+ selectivity, raises the cell current and Na^+ crossover while also decreasing H^+ crossover. This is a preferrable method of improving the electrolyzer's performance but designing a Na^+ selective membrane would be challenging considering the larger Stokes radius of Na^+ compared to H^+ (Luo et al., 2018). Changing the membrane diffusion coefficients does not increase the electric field, and does not activate the Second Wien Effect.

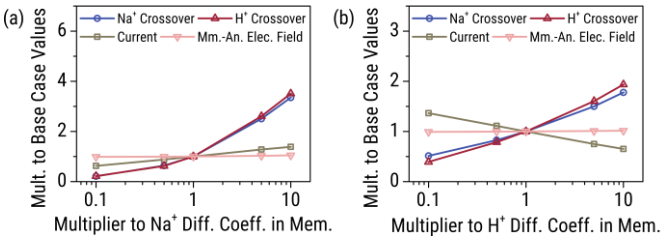

Figure 6: Changes in Na^+ and H^+ crossover, cell current, and electric field at the membrane-anolyte interface at 1 V applied voltage when the Na^+ (a) and H^+ (b) diffusion coefficients in the membrane are varied

4. Conclusions

In this work, we developed a multiphysics model of a batch PEM acid-alkaline electrolyzer to study its operating mechanisms. The model was constructed in COMSOL Multiphysics® and validated with published experimental data. The electric fields and ion flux profiles were derived from the model, and the key reactions and ion transport

mechanisms were inferred. Improvements to the electrolyzer were determined by varying the Na^+ and H^+ membrane diffusion coefficients, then observing the effect on the electrolyzer's performance.
The magnitude of the electric field suggests that the Second Wien Effect is negligible in the electrolyzer, hence electroneutrality is preserved by the crossover of Na^+ from the anolyte to the catholyte. This results in cross-contamination of the electrolytes, so the electrolyzer would require fresh H_2SO_4 and NaOH after each use. Acid-base neutralization occurs to a significant extent but can be minimized by raising the applied voltage, thereby showing a tradeoff between power and reactant usage. Improving the Na^+ selectivity can also reduce acid-base neturalization, but this may not be feasible due to the larger Stokes radius of Na^+ compared to H^+. The model can be utilized for the improvement of acid-alkaline electrolyzer design. In future work, design parameters can be adjusted to minimize the power input. A time-dependent simulation can also be performed.

Nomenclature

c_i – ion concentration, mol m^{-3}
$c_{\mathrm{b},i}$ – bulk ion concentration, mol m^{-3}
E – electric field, V m^{-1}
i – imaginary unit, -
$J_1(x)$ – Bessel function of the first kind of order 1
k_{rep} – replenishment constant, s^{-1}
K_w – water dissociation constant, -
$K_{w,0}$ – water dissociation constant when $|E| = 0$, -
$R_{\mathrm{rep},i}$ – ion replenishment term, mol m^{-3} s^{-1}
T – temperature, K
ε_0 – permittivity of free space, F m^{-1}
ε_r – relative permittivity, -

Acknowledgments

M.T.C would like to acknowledge the Engineering Research and Development for Technology (ERDT) Faculty Research Grant for the financial support. This work is supported by the CIPHER Project (IIID 2018-008) funded by the Commission on Higher Education – Philippine California Advanced Research Institutes (CHED-PCARI).

References

Agar E., Benjamin A., Dennison C.R., Chen D., Hickner M.A., Kumbur E.C., 2014, Reducing capacity fade in vanadium redox flow batteries by altering charging and discharging currents, Journal of Power Sources, 246, 767–774.
Chen T., Mojica F., Li G., Chuang, P.A., 2017, Experimental study and analytical modeling of an alkaline water electrolysis cell, International Journal of Energy Research, 41, 2365–2373.
Eckstrom H.C., Schmelzer C., 1939, The Wien effect: Deviations of electrolytic solutions from Ohm's law under high field strengths, Chemical Reviews, 24, 367–414.
Haynes W.M. (Ed), 2012, CRC Handbook of Chemistry and Physics 93rd ed., CRC Press, Ohio, USA.
Jiang B., Wu L., Yu L., Qiu X., Xi J., 2016, A comparative study of Nafion series membranes for vanadium redox flow batteries, Journal of Membrane Science, 510, 18–26.
Kumar A., Liu X., Lee J., Debnath B., Jadhav A.R., Shao X., Bui V.Q., Hwang Y., Liu Y., Kim M.G., Lee H., 2021, Discovering ultrahigh loading of single-metal-atoms via surface tensile-strain for unprecedented urea electrolysis, Energy and Environmental Science, 14, 6494–6505.
Luo T., Abdu S., Wessling M., 2018, Selectivity of ion exchange membranes: A review, Journal of Membrane Science, 555, 429–454.
Macgillivray A., 1968, Nernst-Planck equations and the electroneutrality and Donnan equilibrium assumptions, The Journal of Chemical Physics, 48, 2903-2907.
Piela P., Wrona P.K., 2006, Some anion-transport properties of Nafion™ 117 from fuel cell hydrogen peroxide generation data, Journal of Power Sources, 158, 1262–1269.
Stenina I.A., Sistat P., Rebrov A.I., Pourcelly G., Yaroslavtsev A.B., 2004, Ion mobility in Nafion-117 membranes, Desalination, 170, 49–57.
Tufa R.A., Chanda D., Tundis L., Hnát J., Bouzek K., Veerman J., Fontananova E., Di Profio G., Curcio E., 2017, Salinity gradient power driven water electrolysis for hydrogen production, Chemical Engineering Transactions, 60, 283–288.
Wang Y., Cho S.C., 2014, Analysis and three-dimensional modeling of vanadium flow batteries, Journal of The Electrochemical Society, 161, A1200–A1212.
Weng S.X., Chen X., 2016, A hybrid electrolyzer splits water at 0.8 V at room temperature, Nano Energy, 19, 138–144.
Zhang H., Wang H., Jiao K., Xuan J., 2020, pH-differential design and operation of electrochemical and photoelectrochemical systems with bipolar membrane, Applied Energy, 268, 115053.
Zhu W., Zhang W., Li Y., Yue Z., Ren M., Zhang Y., Saleh N.M., Wang J., 2018, Energy-efficient 1.67 V single- and 0.90 V dual-electrolyte based overall water-electrolysis devices enabled by a ZIF-L derived acid-base bifunctional cobalt phosphide nanoarray, Journal of Materials Chemistry A, 6, 24277–24284.